Effect of pulsed gas tungsten arc welding on angular distortion in austenitic stainless steel weldments

K. H. Tseng and C. P. Chou

The effect of the parameters of the pulsed gas tungsten arc welding (GTAW) process on the angular distortion in austenitic stainless steel weldments was investigated. Autogenous GTAW was conducted on types 304 and 310 stainless steels to produce a bead on plate weld. The weldment thermal cycle was recorded during pulsed GTAW to investigate the influence of thermal stress. Angular distortion was determined by using the mean vertical displacement method. The experimental results indicate that higher pulse frequency, smaller pulse spacing, greater amplitude ratio, and greater duration ratio can reduce the angular distortion. The angular distortion of type 310 stainless steel weldments was greater than that of type 304 weldments under the same welding conditions because of the lower thermal conductivity and thermal diffusivity of type 310.

STWJ/222

The authors are in the Department of Mechanical Engineering, National Chiao-Tung University, Hsinchu 30049, Taiwan (cpchou@cc.nctu.edu.tw). *Manuscript received 1 October 2000; accepted 5 December 2000.*

INTRODUCTION

Pulsed current welding (PCW) was introduced in the late 1960s as a variant of constant current welding (CCW). The PCW process has many specific advantages over CCW, including enhanced arc stability, increased weld depth/width ratio, narrower heat affected zone (HAZ) range, reduced hot cracking sensitivity, refined grain size, and reduced porosity.[1–6] Pulsed current welding technology has been widely used in fabrication of structures such as aircraft, vehicles, ships, bridges, and pressure vessels or pipes. Switching between predetermined high and low levels of welding current can be used to produce pulsed gas tungsten arc (GTA) welds. Usually, the pulse waves are rectangular in shape (Fig. 1).

The parameters used for pulsed GTA welding (GTAW) are shown in Fig. 1. The main characteristics of PCW are determined by peak current I_P, base current I_B, peak time t_P, and base time t_B. By combining these parameters, the following pulse parameters can be determined:[3,4,7]

(i) pulse frequency $F=(t_P+t_B)^{-1}$
(ii) pulse spacing $S=v(t_P+t_B)$, where v is travel speed
(iii) amplitude ratio $A=I_B/I_P$
(iv) duration ratio $T=t_B/t_P$.

These characteristic pulse parameters can actually control the thermal characteristics and the weld bead geometry.

Austenitic stainless steels are widely used in industrial plant, for example in heat exchangers, nuclear reactors, chemical processing equipment, and gas turbine parts, because of their excellent corrosion resistance, high creep strength, good mechanical strength at high temperature, and high fracture toughness at low temperature. However, austenitic stainless steels have higher thermal expansion coefficient and lower thermal conductivity than carbon or alloy steels and thus a large distortion can be induced after welding fabrication.

During welding, the weldment is locally heated by the arc; thus, the temperature distributions in the weldment are not uniform. Welding temperatures also vary, along with welding times. Typically, the weld metal and base metal near the fusion zone immediately adjoining it are at a temperature substantially above that of the unaffected base metal. During the welding cycle, non-uniform thermal strains are induced in both the weld metal and adjacent base metal. The thermal strains produced during heating are accompanied by plastic upsetting. The non-uniform thermal stresses resulting from these strains combine to produce internal forces that cause welding distortion. It was found that the welding distortions can affect the fabrication, precision (shape and dimensional tolerance), and function (reliability and stability) of the finished structures.

Previous investigations on pulsed GTAW have focused on pulse wave shape,[1] pulse parameters,[3,4,7–10] and the effect of pulsed GTAW on microstructures or mechanical properties of the weldment.[2,6,11] Studies of the influence of pulsed GTAW on weldment distortion have been limited. Because distortions during welding are unavoidable, the effects of the welding process on the distortion in finished structures cannot be disregarded. For this reason, finding means of reducing distortion is important.

In the present work, detailed experiments were conducted to investigate the effect of pulsed GTAW parameters on angular distortion in austenitic stainless steel weldments.

EXPERIMENTAL

Austenitic stainless steels 304 and 310 having the chemical compositions and mechanical properties listed in Table 1 were used. Plates 8 mm in thickness were cut into strips of

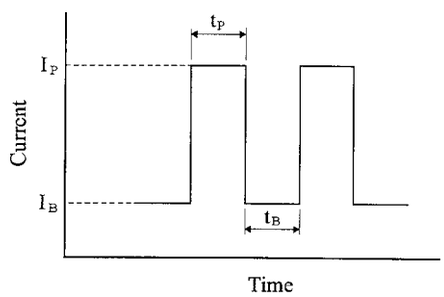

1 Parameters used for pulsed GTAW: peak current I_P, base current I_B, peak time t_P, and base time t_B

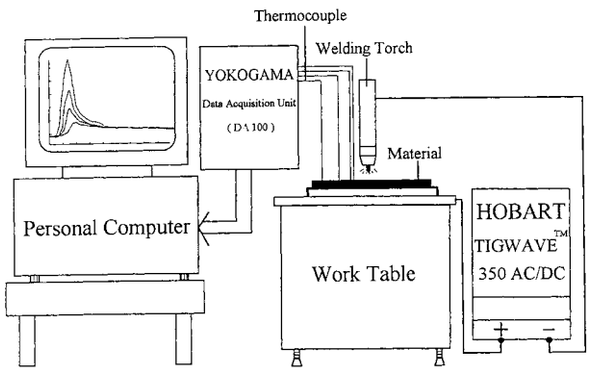

2 Schematic illustration of thermal cycle recording system

size 130×130 mm, which were roughly polished with 400 grit abrasive paper to remove surface impurities, then cleaned with acetone. Autogenous GTAW was conducted with a standard 2% thoriated tungsten electrode. The electrode tip configuration was a blunt point with a 90° included angle. The argon shielding gas flowrate was 10 L min^{-1}.

A thermocouple, separately attached 2 mm from the fusion line of each weld, was used to record the weldment thermal cycle. The recording equipment (Fig. 2) included a dynamic temperature measurement system and a chromel/alumel thermocouple.

The mean vertical displacement method was used to measure the welding distortion, as schematically illustrated in Fig. 3*a*. A position fixed hole is drilled at the back of points P_1, P_2, and P_3, and a pillar is attached to each hole. Three pillars (one stable, the other two adjustable) were used to adjust the horizontal level. The distance from each point to the horizontal surface was recorded. Measurements were taken both before and after welding. The difference between the measurements before and after welding gave the vertical displacement caused by welding, and the angular distortion U can be derived from this mean vertical displacement as

$$|U| = [(A+B)-(C+D)]/2$$

where A, B, C, and D are the mean vertical displacement values of each point, as shown in Fig. 3*b*.

Metallographic transverse sections of the weld beads were prepared to display the fusion zone, HAZ, and unaffected base metal microstructures. An optical microscope was used to measure the dimensions of the weld bead geometry (weld depth/width ratio and HAZ range). All metallographic specimens were prepared by mechanical lapping, grinding, and polishing to a 0·3 μm finish, followed by etching in a solution of 10 g $CuSO_4$ + 50 mL HCl + 50 mL H_2O.

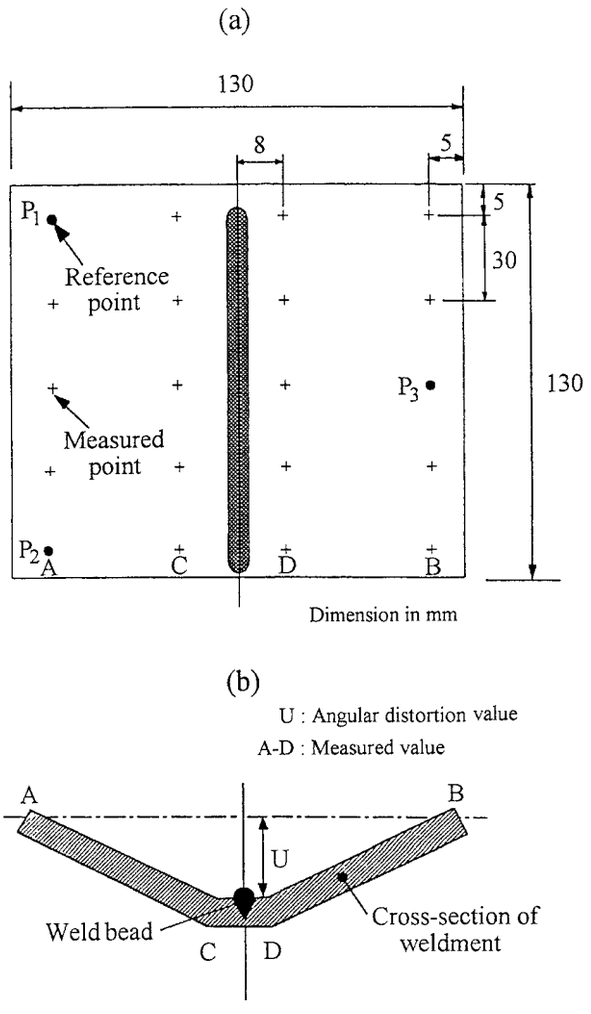

3 Schematic illustration of mean vertical displacement method

RESULTS AND DISCUSSION

The welding parameters used are presented in Table 2. Average welding current, arc voltage, and travel speed were all kept constant, i.e. the heat input per unit length in a weld is fixed, while pulse frequency, pulse spacing, amplitude ratio, and duration ratio during pulsed GTAW were varied.

Effect of pulse frequency

The effect of pulse frequency on angular distortion for constant heat input per unit length, amplitude ratio, and duration ratio is shown in Fig. 4. It can be seen that angular distortion is decreased with increasing pulse frequency. The measured weld bead geometry during pulsed GTAW (Figs. 5 and 6) can be used to explain this result. It is observed that higher pulse frequency tends to increase the weld depth/width ratio and reduce the HAZ range of the weld beads. According to previous investigations,[12,13] greater weld depth/width ratio and narrower HAZ range are characteristic of increased energy density of the welding heat source. On the basis of the present experimental results, higher pulse frequency during pulsed GTAW can enhance the energy density of the heat source, and therefore the

Table 1 Chemical composition and mechanical properties of experimental austenitic stainless steels

	Composition, wt-%									
Material	C	Si	Mn	P	S	Cr	Ni	Yield strength, MPa	Elastic modulus, GPa	Poisson ratio
SUS304	⩽0·08	0·44	0·95	⩽0·04	⩽0·04	18·7	8·16	290	193	0·25
SUS310	⩽0·20	0·79	1·64	⩽0·04	⩽0·04	23·9	19·61	311	204	0·32

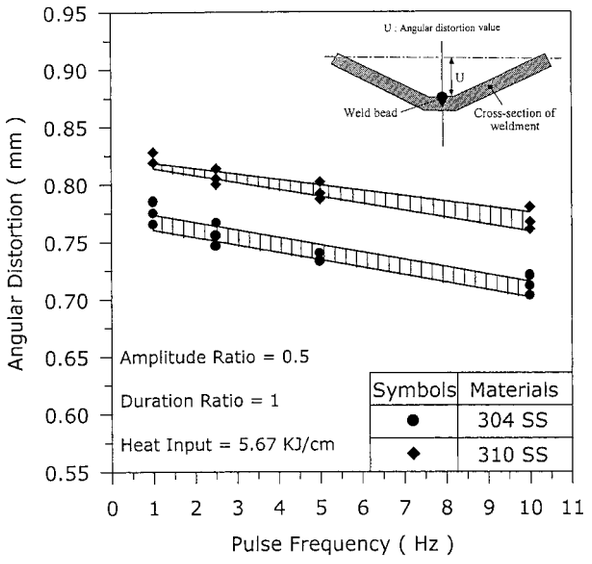

4 Angular distortion as function of pulse frequency during pulsed GTAW

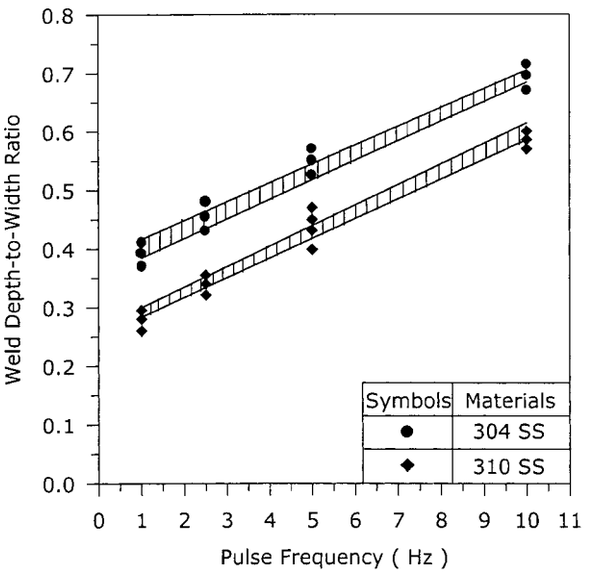

5 Effect of pulse frequency on weld depth/width ratio in austenitic stainless steel weld metals

angular distortion of austenitic stainless steel weldments can be reduced.

Effect of pulse spacing

The influence of varying pulse spacing on angular distortion is shown in Fig. 7. As the pulse spacing increases, the angular distortion of the weldments is increased. In the present study, the heat input per unit length is kept constant, and thus cannot effect any change in angular distortion. The pulse spacing is proportional to (t_P+t_B), whereas the pulse frequency is inversely proportional to (t_P+t_B) for the same heat input per unit length. It can be seen therefore that the pulse spacing and pulse frequency exhibit opposite experimental trends.

Table 2 Welding parameters for autogenous GTAW experiments

I_P, A	I_B, A	t_P, s	t_B, s	I_{ave}*, A	E†, V	v, cm min^{-1}	Q‡, kJ cm^{-1}
Designated parameters used to vary pulse frequency and pulse spacing							
150	75	0·5	0·5	112·5	12·6	15	5·67
150	75	0·2	0·2	112·5	12·6	15	5·67
150	75	0·1	0·1	112·5	12·6	15	5·67
150	75	0·05	0·05	112·5	12·6	15	5·67
Designated parameters used to vary amplitude ratio							
180	45	0·1	0·1	112·5	12·6	15	5·67
165	60	0·1	0·1	112·5	12·6	15	5·67
150	75	0·1	0·1	112·5	12·6	15	5·67
135	90	0·1	0·1	112·5	12·6	15	5·67
120	105	0·1	0·1	112·5	12·6	15	5·67
Designated parameters used to vary duration ratio							
180	90	0·1	0·3	112·5	12·6	15	5·67
150	75	0·2	0·2	112·5	12·6	15	5·67
128·6	64·3	0·3	0·1	112·5	12·6	15	5·67

*Average welding current I_{ave} defined as $(I_Pt_P+I_Bt_B)/(t_P+t_B)$.
†Arc voltage E cannot be measured directly. However, if the arc length, welding current, travel speed, gas flowrate, and electrode geometry are constant for each weld, then the variation of arc voltage between welds should not be great enough to affect the heat input calculation for a comparative study such as the present one. The value of arc voltage used for calculation purposes is 12·6 V, which is the value obtained in conventional GTAW on test specimens using the same arc length of 2·5 mm, welding current of 112·5 A, travel speed of 15 cm min^{-1}, and gas flowrate of 10 L min^{-1} used for pulsed GTAW process in present study.
‡Heat input per unit length $Q=60(I_Pt_P+I_Bt_B)E/(t_P+t_B)v$ J cm^{-1}.

Effect of amplitude ratio

It can be seen in Fig. 8 that welding angular distortion decreases as the pulse amplitude ratio increases. The result is related to the weldment thermal cycle (Fig. 9). During pulsed GTAW, a greater amplitude ratio can reduce the temperature difference between the fusion zone and unaffected base metal zone in the weldment. According to previous work, the magnitude of the shrinkage stresses is reduced by reductions in the temperature gradient.[14,15] Therefore, a greater amplitude ratio can reduce the temperature gradient in the weldment, and hence welding angular distortion.

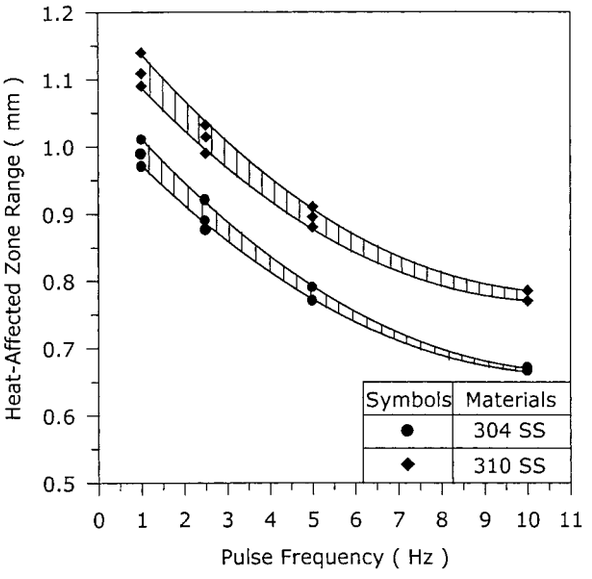

6 Effect of pulse frequency on HAZ range in austenitic stainless steel weld metals

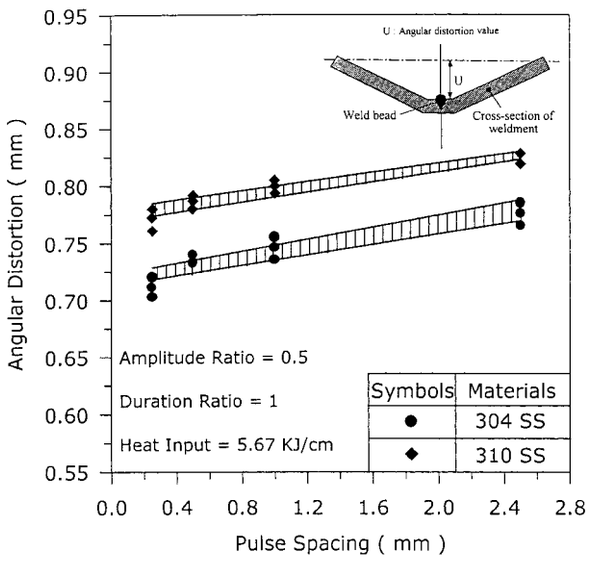

7 Angular distortion as function of pulse spacing during pulsed GTAW

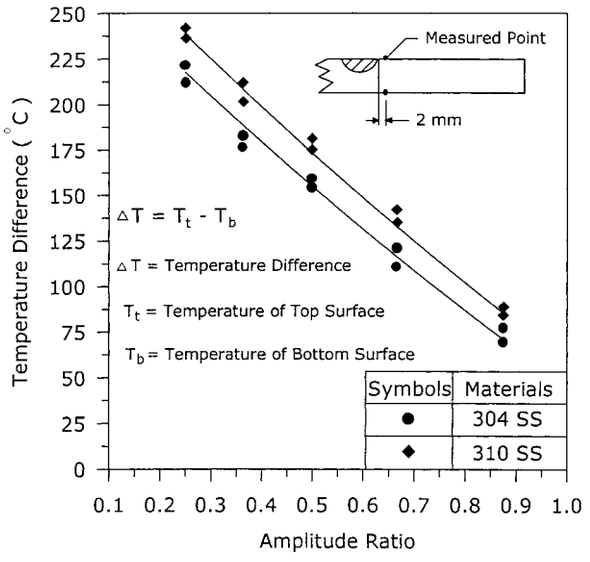

9 Effect of amplitude ratio on temperature difference in austenitic stainless steel weldments

Effect of duration ratio

As the duration ratio increases, the angular distortion of the weldment is decreased (Fig. 10). This result is also related to the weldment thermal cycle, as shown in Fig. 11: as the duration ratio increases, the peak temperature of the thermal cycle is reduced. Lin and co-workers[15–17] have reported that welding thermal stress increases with increasing peak temperature during welding, i.e. lower thermal cycle peak temperatures obtained by using a higher duration ratio during GTAW can reduce angular distortion of the weldment.

Effect of steel composition

The present experimental results clearly indicate that the angular distortion of type 310 stainless steel weldments is larger than that of type 304 under the same welding conditions. The experimental results can be analysed from the thermophysical properties of the materials used.

Types 304 and 310 stainless steels have almost the same coefficient of thermal expansion (Table 3); therefore, the effect of this variable on distortion can be neglected. However, type 310 has a lower thermal conductivity. In general, a lower thermal conductivity will increase the temperature difference between the fusion zone and unaffected base metal in the weldment, and therefore the welding distortion will be increased.

It can also be seen from the data in Table 3 that type 310 stainless steel has a lower thermal diffusivity than type 304. Thermal diffusivity can be considered as a measure of the ability of a material to store heat. Usually, a lower thermal diffusivity suggests a higher capacity to store heat and will raise the peak temperature of the weldment thermal cycle, thus increasing the distortion of the weldment.

Normally, the microstructure of these stainless steels is fully austenitic at room temperature. During normal welding processes, the cooling rate is so rapid that the ferrite–austenite transformation does not proceed to

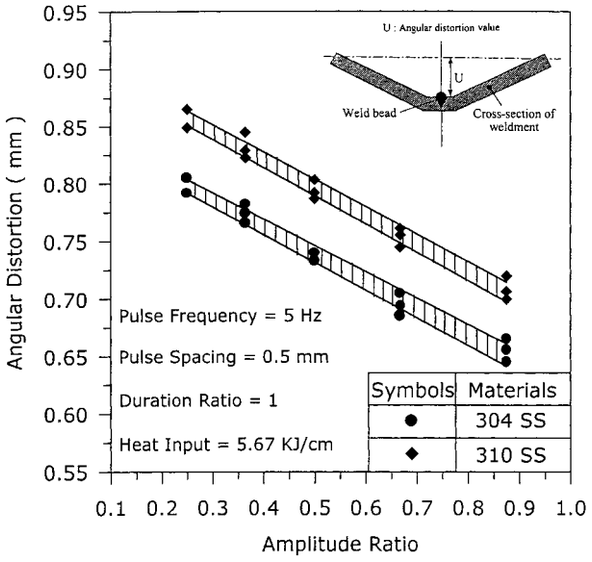

8 Angular distortion as function of amplitude ratio during pulsed GTAW

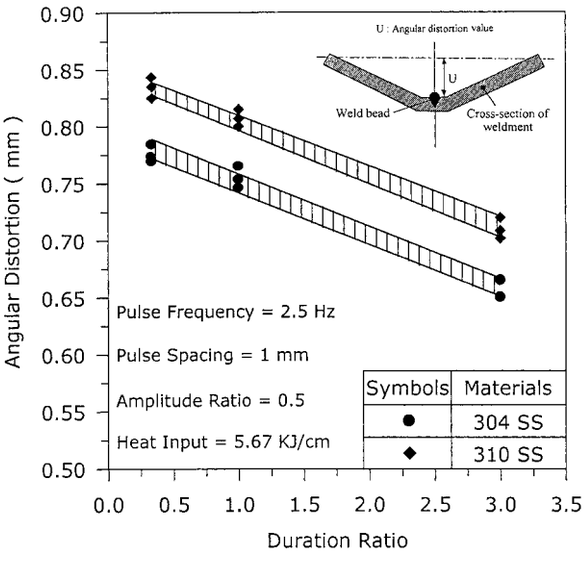

10 Angular distortion as function of duration ratio during pulsed GTAW

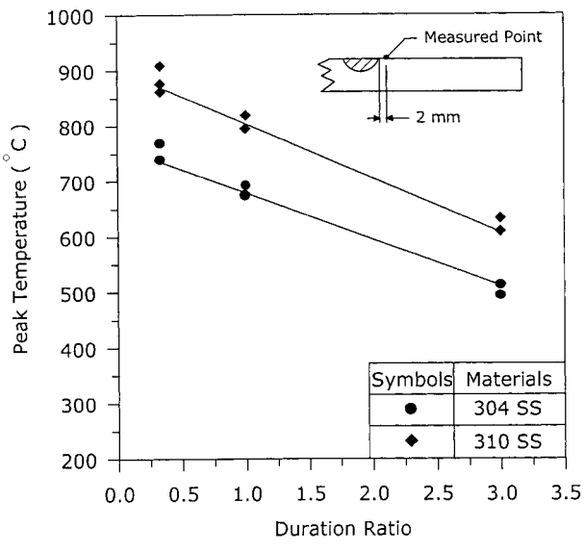

11 Effect of duration ratio on peak temperature in austenitic stainless steel weldments

completion, and some δ-ferrite is retained at room temperature after solidification. Thus, the final microstructure in austenitic stainless steel weld metals is a duplex $\delta+\gamma$ structure. The properties of austenitic stainless steel weld metals are strongly influenced by the presence of δ-ferrite.[18] Several studies have indicated that a certain amount of retained δ-ferrite in austenitic stainless steel welds can be beneficial in preventing hot cracking in as welded structures.[19–21] Two explanations were proposed to explain the beneficial effect of the retained δ-ferrite structure in reducing welding distortion.

The first explanation is based on the fact that δ-ferrite has a greater high temperature ductility than austenite and therefore δ-ferrite within the austenitic matrix can moderate the action of thermal stress during welding. The second explanation can be related to the fact that welding distortion is reduced because the bcc ferrite structure has a smaller coefficient of thermal expansion than the fcc austenite structure, and thereby shrinkage stresses during cooling are reduced.

To summarise, because type 310 stainless steel has a lower thermal conductivity and thermal diffusivity, greater temperature gradients and higher peak temperatures can be induced during welding, compared with those in type 304. Therefore, the angular distortion of type 310 stainless steel weldments is greater. In addition, the existence of retained δ-ferrite within the austenitic matrix has a beneficial effect in reducing welding distortion in austenitic stainless steels.

Table 3 Thermophysical properties of austenitic stainless steels

Material	Coefficient of thermal expansion, K^{-1}	Thermal conductivity, $W\ m^{-1}\ K^{-1}$	Thermal diffusivity*, $m^2\ s^{-1}$
SUS304	$17{\cdot}0\times10^{-6}$	16·3	$4{\cdot}1\times10^{-6}$
SUS310	$16{\cdot}1\times10^{-6}$	14·1	$3{\cdot}6\times10^{-6}$

*Thermal diffusivity $=k/\rho C_P$, where k is thermal conductivity, ρ density, and C_P specific heat capacity.

CONCLUSIONS

1. During pulsed GTAW, higher pulse frequency or smaller pulse spacing can enhance the energy density of the welding heat source, thereby reducing the angular distortion of austenitic stainless steel weldments.
2. Greater pulse amplitude ratio can reduce the temperature difference between the fusion zone and unaffected base metal zone in the weldment, and thus angular distortion.
3. Lower thermal cycle peak temperatures can be obtained by using a greater pulse duration ratio. This also reduces angular distortion of the weldment.
4. Because type 310 stainless steel has a lower thermal conductivity and thermal diffusivity than type 304, greater temperature gradients and higher peak temperatures can be induced during the welding cycle. As a result, the angular distortion in type 310 is greater.
5. The existence of retained δ-ferrite within the austenitic matrix also has a beneficial effect in reducing welding distortion.

REFERENCES

1. W. TROYER, M. TOMSIC, and R. BARHORST: *Weld. J.*, 1977, **56**, (1), 26–32.
2. D. W. BECKER and C. M. ADAMS: *Weld. J.*, 1979, **58**, (5), 143s–152s.
3. D. W. BECKER and C. M. ADAMS: *Weld. J.*, 1978, **57**, (5), 134s–138s.
4. A. A. OMAR and C. D. LUNDIN: *Weld. J.*, 1979, **58**, (4), 97s–104s.
5. C. F. TSENG and W. F. SAVAGE: *Weld. J.*, 1971, **50**, (11), 777–786.
6. Y. SHARIR, J. PELLEG, and A. GRILL: *Met. Technol.*, 1978, **5**, 190–196.
7. C. L. TSAI and C. A. HOU: *J. Heat Transfer*, 1988, **110**, 160–165.
8. S. RAJASEKARAN, S. D. KULKARNI, U. D. MALLYA, and R. C. CHATURVEDI: *Weld. J.*, 1998, **77**, (6), 254s–269s.
9. A. J. R. AENDENROOMER and G. DEN OUDEN: *Weld. J.*, 1998, **77**, (5), 181s–187s.
10. R. E. LEITNER, G. H. MCELHINNEY, and E. L. PRUITT: *Weld. J.*, 1973, **52**, (9), 405s–410s.
11. G. M. REDDY, A. A. GOKHALE, and K. PRASAD RAO: *Mater. Sci. Technol.*, 1998, **14**, 61–66.
12. D. E. POWERS, R. F. DUHAMEL, P. ANTHONY, D. A. BELFORTE, K. W. CARLSON, L. S. DEROSE, D. ELZA, D. GUSTAFERRI, A. LINGENFELTER, and R. W. WALKER: in 'Welding handbook', (ed. R. L. O'Brien), 8th edn, Vol. 2, 714–738; 1991, Miami, FL, American Welding Society.
13. H. B. CARY: 'Modern welding technology', 4th edn, 237–264; 1998, Englewood Cliffs, NJ, Prentice-Hall.
14. K. MASUBUCHI: 'Analysis of welded structures', 1st edn, 60–87; 1980, Oxford, Pergamon Press.
15. Y. C. LIN and K. H. LEE: *J. Mater. Process. Technol.*, 1997, **63**, 797–801.
16. Y. C. LIN and J. Y. PERNG: *Sci. Technol. Weld. Joining*, 1997, **2**, 129–132.
17. Y. C. LIN and K. H. LEE: *Int. J. Pressure Vessels Piping*, 1997, **71**, 197–202.
18. M. H. CHEN and C. P. CHOU: *Sci. Technol. Weld. Joining*, 1999, **4**, 58–62.
19. F. C. HULL: *Weld. J.*, 1967, **46**, (9), 399s–409s.
20. W. T. DELONG: *Weld. J.*, 1974, **53**, (7), 273s–286s.
21. G. L. LEONE and H. W. KERR: *Weld. J.*, 1982, **61**, (1), 13s–21s.